

Science with Soft X-Rays

“But, soft! What light ... ”
Romeo and Juliet

High brightness synchrotron radiation in the soft x-ray and ultraviolet regions offers improved spectral resolving power, spatial resolution, and coherence. Examples are presented of science being done in the areas of wet cell biology, condensed matter physics and extreme ultraviolet optics technology.

Neville Smith

Introduction

Users of synchrotron radiation fall into two fairly distinct camps: users of the soft x-ray and vacuum ultraviolet (VUV) region of the spectrum; and users of the hard x-ray region. The distinction can be expressed quantitatively by comparing the energies of a photon and an electron whose wavelengths are one Ångstrom. The scientific question posed by the users of hard x-rays tends to be “where are the atoms?” with much emphasis on the determination of crystal structures and molecular structures using techniques such as x-ray diffraction. The probing *photon* should therefore have a wavelength comparable to interatomic distances. With $\lambda = 1 \text{ Å}$, we have:

$$E (\text{photon}) = hc / \lambda \approx 12.4 \text{ keV}.$$

In the soft x-ray/VUV region, on the other hand, the question tends to be “what are the electrons doing as they migrate between the atoms?” The emphasis turns to studies of chemical bonding and valence band structures using techniques such as photoemission and spectroscopy. It is now desirable that the *photoelectron* should have a wavelength comparable to interatomic distances. With $\lambda = 1 \text{ Å}$, we have

$$E (\text{electron}) = h^2 / 2 m \lambda^2 \approx 150 \text{ eV}.$$

Photoemission investigations of valence bands and energy-momentum or $E(\mathbf{k})$, relations are generally done using photon energies below 100 eV. Indeed, it is possible to scan the photoelectron wavevector out to the Brillouin zone boundary using photon energies as low as 20 eV.

This natural separation into two energy regions is reflected in the establishment in the United States of two new synchrotron radiation facilities, the Advanced Photon Source (APS) at the Argonne National Laboratory optimized for delivery of hard x-rays, and the Advanced Light Source (ALS) at the Lawrence Berkeley National Laboratory optimized for soft x-ray/VUV science. These sources have been designed for high brightness.

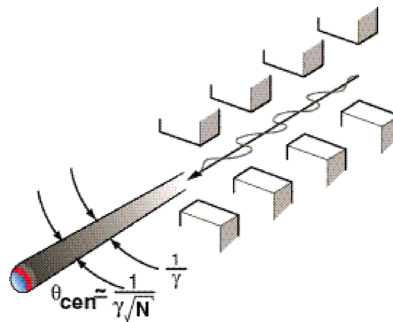
Between the two extremes lies the “soft x-ray” region (100-1000 eV) which contains the binding energies of core levels of important elements, especially the first row of the periodic table. The binding energies of the 1s core level in C, N, and O are 290 eV, 400 eV, and 530 eV respectively. These elements have only one core level, and so core-level spectroscopy of these elements must be done in the soft x-ray region. This region also contains the L-edges (2p core level to 3d valence level) of the transition metals. Particularly important are the L-edges of the elemental ferromagnets, Fe (710 eV), Co (780 eV), and Ni (850 eV). In addition, the cuprate high-temperature superconductors and the manganate CMR (colossal magnetoresistance) materials have propelled the L-edges of Cu (930 eV) and Mn (640 eV) into prominence.

The intent of this article is to outline science being done using the soft x-ray and VUV part of the spectrum, with emphasis on the new opportunities offered by the high brightness of the ALS and its sister facilities elsewhere in the world. High brightness has three main advantages (See Box), and our examples have been chosen to illustrate these three advantages. For reasons of familiarity, the examples chosen will be taken from work done at the ALS and at the NSLS (National Synchrotron Light Source) at Brookhaven. Similar work is being done at the other sources, such as ELETTRA (Trieste), MAX-Lab (Lund), and BESSY-II (Berlin), and SRC (Madison), as well as facilities with moderately higher energy such as SSRL (Stanford).

Box

The Brightness Advantage

The third generation synchrotron radiation sources have been designed for high brightness, sometimes called brilliance. The highest brightness is achieved with the use of “undulators”, periodic magnetic structures that force the electrons in the synchrotron storage ring to oscillate about their central trajectory. The cumulative effect of many such undulations is to produce a beam of radiation in a very narrow angular cone about the forward direction. This, combined with the inherent smallness ($30\mu\text{m} \times 200\mu\text{m}$) of the electron source in the ring, is the brightness advantage. For further reading, see D. Attwood, “Soft X-rays and Extreme Ultraviolet Radiation”, Cambridge University Press (2000).



But what does brightness really buy you? Through a perfect optical system brightness is a conserved quantity which means that it is possible to put a lot of light into a small spot. This has three practical consequences:

- *Small spot on the sample.* Techniques (spectroscopy, diffraction, etc.) can now be performed with fine spatial resolution. With demagnifying mirrors, micron and submicron spot sizes can be achieved spawning a variety of x-ray microscopes. With use of Fresnel zone plates, spot sizes of 30nm are routine and 10nm should be possible.
- *Narrow slits.* With small spot size it is possible to cram a lot of light through very narrow slits of a monochromator or spectrometer. Brightness can therefore be traded for high resolving power, thereby driving a basic research program with much emphasis on strongly correlated electron systems in both the condensed state and gas phase.
- *Tiny pinholes.* It is likewise possible to cram a lot of light through tiny pinholes, thereby generating perfect spherical waves of high amplitude. This is the property of spatial coherence which can be exploited for interferometry, speckle and dynamic scattering experiments.

Spatial Resolution: Wet and Dry Soft X-ray Microscopy

An important feature of the soft x-ray region is the “water-window”, the photon energy range between the carbon K-edge (290eV) and the oxygen K-edge (530eV). In this range, organic matter (i.e. carbon) is absorbing whereas water (i.e. oxygen) is relatively transparent. This provides a contrast mechanism which permits microscopic analysis of cells in their natural aqueous environment. The richness of carbon near-edge spectra provides a chemical fingerprint, which serves as yet another contrast mechanism in the microscopic investigation of systems like polymer blends, which are of critical industry importance to the chemical industry. Let us focus first on an example of wet cell biology.

Confocal microscopy in the visible region is a powerful and widely used technique in cell biology. Its spatial resolution is limited by the wavelength of light. With use of Fresnel zone plates as focussing elements in the water window, it is possible to see features 5-10 times smaller than in the optical confocal microscope. Indeed the large potential impact of soft x-ray microscope on biology was one of the driving forces behind the building of low-energy third generation synchrotron radiation facilities. It is only recently, however, that this dream has started to come true.

A team of cell biologists working under the leadership of Carolyn Larabell is addressing the frontier problem of the localization, co-localization, and redistribution of proteins as they perform their functions in cells. Figure 1 shows mouse 3T3 fibroblasts taken with a spatial resolution of 25nm [1]. The sample was taken freshly from culture and cryofixed (i.e. frozen with liquid-nitrogen cooled helium gas) and, therefore, the cells more closely resemble their native state than do chemically fixed cells. Using this approach, the cellular ultrastructure is extremely well preserved and is revealed with a unique combination of high spatial resolution and good contrast. Numerous organelles, granules of various sizes, and tubular structures such as mitochondria are readily seen in the cytoplasm. Even the contents of the nucleus, which is approximately 5- μ m thick in these cells, can be visualized without the need for physically sectioning the cell. Nuclear structures such as the nucleoli, which are densely packed with RNA, appear as dense bodies and the nuclear envelope, a double-layered membrane encircling the entire nucleus, appears as a distinct line encircling the nucleus. The striking contrast of the cellular ultrastructure is derived from imaging in the water window; these cells had not been exposed to any chemical fixatives or contrast enhancement agents. Due to the unique differential contrast provided by x-ray imaging, the location of specific proteins and nucleic acids is readily identified using gold-tagged labels that are easily distinguished from biological constituents [1]. Future developments will include collection of images at different tilt angles followed by tomographic reconstructions to restore the three-dimensional information. The use of X-ray microscopy is rapidly emerging as an important tool for determining structure-function relationships of proteins and cells. The future use of zone plate lenses with better resolution will enhance the information generated using this approach.

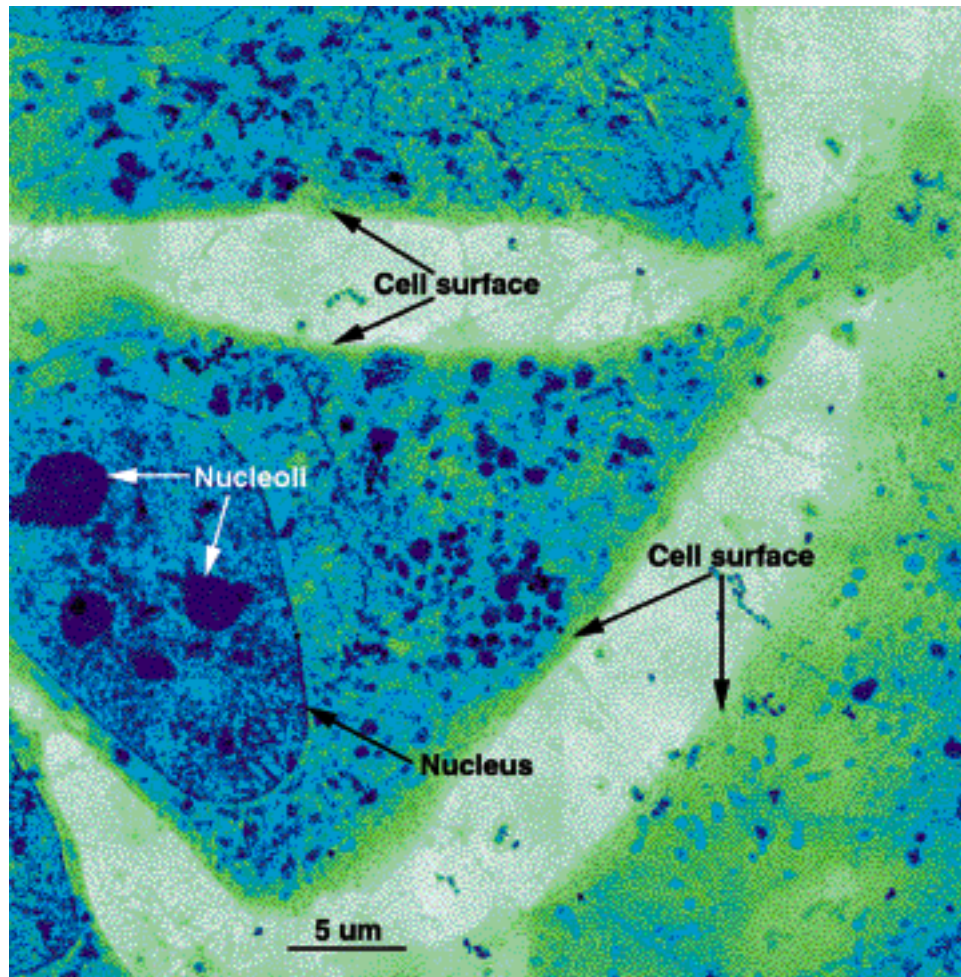


FIGURE 1. Soft x-ray transmission micrograph of mouse 3T3 fibroblasts. The data were taken in the “water window” with a spatial resolution of 30nm permitting observation of features such as nucleoli and the sharp nuclear membrane not resolvable with optical confocal microscopy. (Courtesy C. Larabell)

Fresnel zone plates represent only one of the ways to achieve fine spatial resolution. Another way is to use electron optics rather than photon optics. In photoelectron emission microscopy (PEEM) the principle is to illuminate an area on the sample and then to pass the ejected photoelectrons through an electron-microscope column to produce an enlarged image of the illuminated spot. Since the detected particles are electrons, the experiment must be done in vacuum thereby precluding the investigation of wet samples. Nevertheless, there are plenty of dry systems of interest.

Fritjof Nolting and collaborators [2] have recently addressed the unresolved problem of exchange bias, i.e. the alignment of ferromagnetic spins by an antiferromagnet. This is something of an old chestnut in condensed matter physics, but has assumed considerable recent importance because of its relevance to the artificial magnetic layered structures used in the manufacture of devices such as magnetic read heads and magnetic memory cells. To build such a magnetic structure, it has proved necessary to use an antiferromagnetic material as a substrate in order to pin the orientation of the first ferromagnetic layer. The mechanism is not well understood. By a very artful switch between two contrast mechanisms, linear dichroism for antiferromagnetic contrast and circular dichroism for ferromagnetic contrast, Nolting et al have provided what has hitherto been lacking, an incisive technique to study the problem.

The system chosen for study was thin ferromagnetic film of Co on an antiferromagnetic substrate of LaFeO_3 . Figure 2 shows the PEEM micrographs and spectra. Linear dichroism (difference in the absorption of linearly polarized x-rays with the antiferromagnetic axis parallel or perpendicular to the electric vector of the light) at the Fe L-edge provides sufficient contrast to distinguish the vertically and horizontally oriented antiferromagnetic domains. Switching to circular dichroism (difference in absorption between left and right circularly polarized photons) at the Co L-edge, it can be seen that the ferromagnetic domains are indeed aligned with the domains of the antiferromagnetic substrate with the ferromagnetic magnetization pointing in either direction. It is then possible with PEEM to zoom in on specific areas and measure the magnetization reversal. This can be done as a function of temperature and, eventually, using the pulsed nature of synchrotron radiation, it will be done as a function of time. The present spatial resolution of PEEM is 20nm, but it is expected that aberration corrected instruments being developed in the U.S. and Germany will reduce this to 2nm.

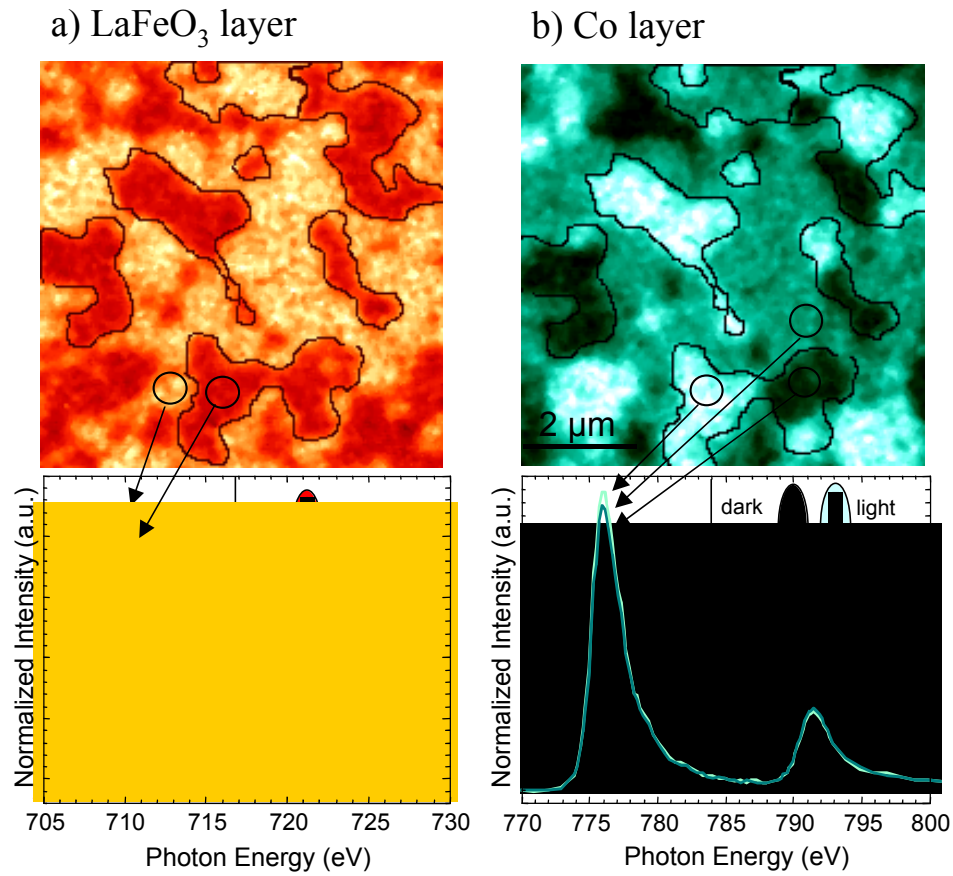


FIGURE 2. Images and local spectra from a ferromagnetic Co layer on an antiferromagnetic LaFeO₃ substrate. (a) Antiferromagnetic contrast is obtained at the Fe L-edge using linear dichroism, the difference in absorption between parallel and perpendicular orientation of the antiferromagnetic axis and the electric vector of the light. (b) Ferromagnetic contrast at the Co L-edge using circular dichroism, the difference in absorption between left and right circular polarization. Note that the ferromagnetic Co domains align with the substrate antiferromagnetic domains, but can split into subdomains of opposite magnetization. (Courtesy S. Anders.)

Spectral Resolving Power: Electronic Structure of High T_c Superconductors

One of the most tantalizing problems in condensed-matter physics is the origin of high temperature superconductivity. Phil Anderson has declared [4] that angle-resolved photoemission spectroscopy (ARPES) will provide the smoking gun and “is, for this problem, the experiment that will play the role that tunneling played for BCS.” Great strides have indeed been made. ARPES experiments have revealed the d-wave nature of the superconductive coupling mechanism [5] and the existence of a “pseudogap”. Attention has turned recently to the existence of stripes [6] and we discuss here some ARPES experiments by Zhi-xun Shen and co-workers [7] which make a connection between stripes and the Fermi surface, i.e. the boundary in k-space separating the occupied and unoccupied electronic states.

The experiments were done on a model cuprate compound ($\text{La}_{1.28}\text{Nd}_{0.6}\text{Sr}_{0.12}\text{CuO}_4$ (Nd-LSCO). This remarkable compound has the one-eighth ($\text{Sr}_{0.12}$) strontium doping at which superconductivity is actually suppressed. The replacement of some La with Nd serves to stabilize the stripe phase which consists, at this doping, of rows of charge carriers separate by triple rows of antiferromagnetically ordered spins whose ordering flips phase across the charge stripes. (See Figure 3). Shen et al extract a Fermi surface by integrating the photoemission spectra over an energy range near the Fermi level to obtain electron momentum density maps that reveal the Fermi surface information. The Fermi surface displays the shape of a cross, although it is thought that this is the superposition of two bars corresponding to domains having the two alternative orientations of the stripes. The boundaries of the bars are given by $|k_x| \leq \pi/4$ and $|k_y| \leq \pi/4$ implying that the electron system is highly one-dimensional consistent with the fourfold periodicity and the one-eighth doping. The data are inconsistent with the more rounded Fermi surface based on the two-dimensional copper-oxygen planes.

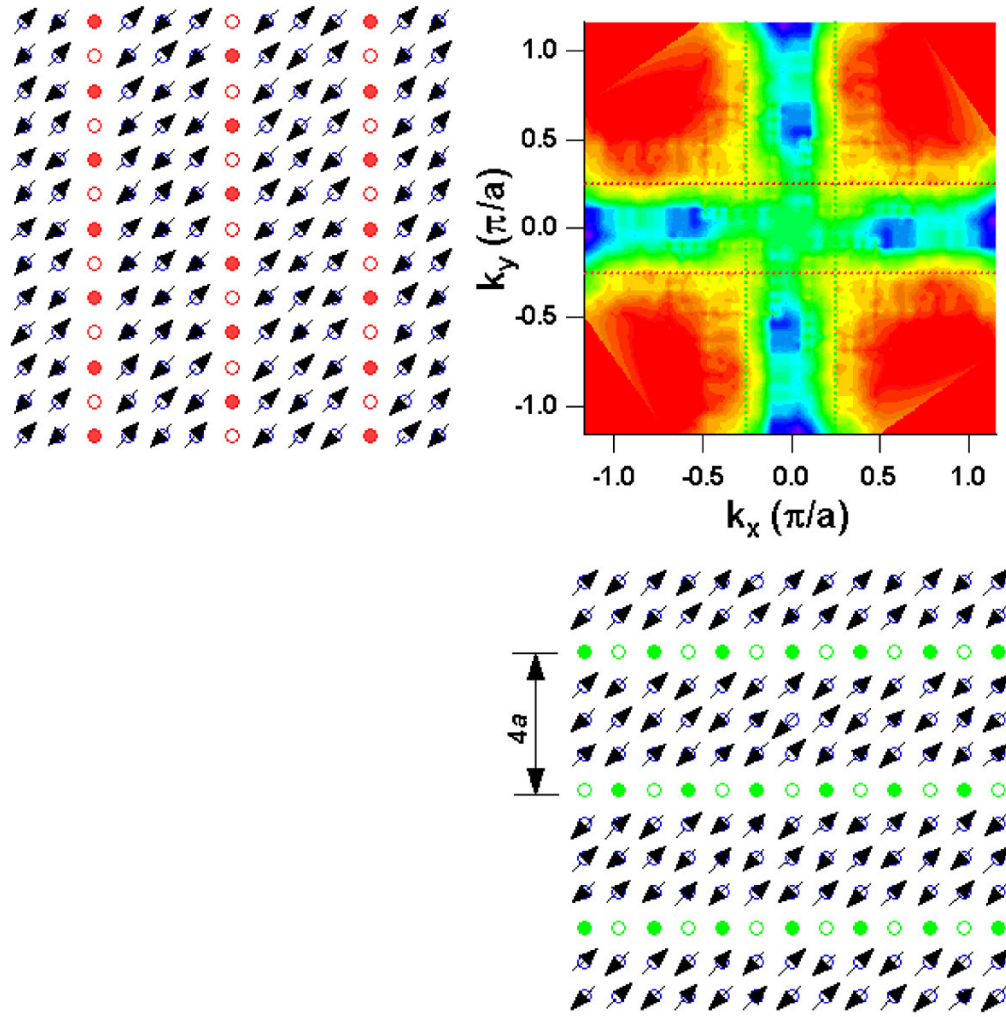


FIGURE 3. Fermiology meets stripology. In the stabilized stripe phase, rows of charge carrying atoms are separated by triple-rows of antiferromagnetic material with a π phase slip across the charge carrying rows. The “Maltese Cross” Fermi surface (upper right) is confined within $|k_x| \leq \pi/4$ and $|k_y| \leq \pi/4$ consistent with a superposition of the two alternative domain orientations of the stripe phase.

High resolving power is permitting photoemission spectroscopists to approach ever closer to the Fermi level, E_F . Energy band structures ($E(\mathbf{k})$ relations) can now be measured with great precision. For example, the long anticipated kink in the $E(\mathbf{k})$ relation close to E_F due to the electron-phonon interaction has now been observed by a number of groups. Attention has turned also to the lifetime width of peaks in the photoemission spectra. The energy dependence of the lifetime width in the vicinity of E_F is a strong indicator of Fermi-liquid or non-Fermi-liquid like behavior.

The measured photoelectron energy spectrum at a given angle of emission is proportional to the spectral function given by

$$A(\mathbf{k}, \omega) \propto \frac{\text{Im} \Sigma(\mathbf{k}, \omega)}{[\omega - E_k - \text{Re} \Sigma(\mathbf{k}, \omega)]^2 + [\text{Im} \Sigma(\mathbf{k}, \omega)]^2}$$

where $\text{Re} \Sigma(\mathbf{k}, \omega)$ and $\text{Im} \Sigma(\mathbf{k}, \omega)$ are the real and imaginary parts of the self energy. Modern state-of-the-art photoemission spectrometers display in parallel two dimensions of information, photoelectron energy and angle. Peter Johnson and his collaborators, working at the Brookhaven National Synchrotron Light Source, have shown that the cleanest cut through this space for the determination of the $\text{Im} \Sigma$ is the momentum distribution curve (MDC) which is the photoemission intensity as a function of momentum k at constant excitation energy ω . The MDC's are immune from the distorting effects of the Fermi function and the inelastic background to the spectra.

Figure 4 shows a comparison of lifetime widths measured by Johnson's group on optimally doped $\text{Bi}_2 \text{Sr}_2 \text{CaCu}_2 \text{O}_{8+\delta}$ (Bi2212) with those measured on testbed system, a molybdenum surface state [8]. Since the measurement of photoemission line widths is fraught with experimental artifacts, it is highly desirable to test the method on a well-understood system. A well established surface state on the Mo(110) surface provides such a test bed system. The ω dependence of the $\text{Im} \Sigma$ is well described by a contribution due to the electron-phonon interaction plus a ω^2 term characteristic of a Landau Fermi liquid. By contrast, the measurements of $\text{Im} \Sigma$ for Bi2212 are clearly inconsistent with Fermi-liquid behavior. First, the data lie above the curve $\omega = |2\text{Im} \Sigma|$ whereas the validity of Fermi liquid theory requires $|2\text{Im} \Sigma| < \omega$. Second, the ω dependence and T dependence of the self energy suggest that the system exhibits quantum critical behavior. This interpretation, as well as the discussion above concerning the stripe phase, remains controversial. The important conclusion for the purpose of this article is that the incisiveness of ARPES does indeed look likely to provide Anderson's smoking gun, and that the work requires high brightness synchrotron radiation in the vacuum ultraviolet region.

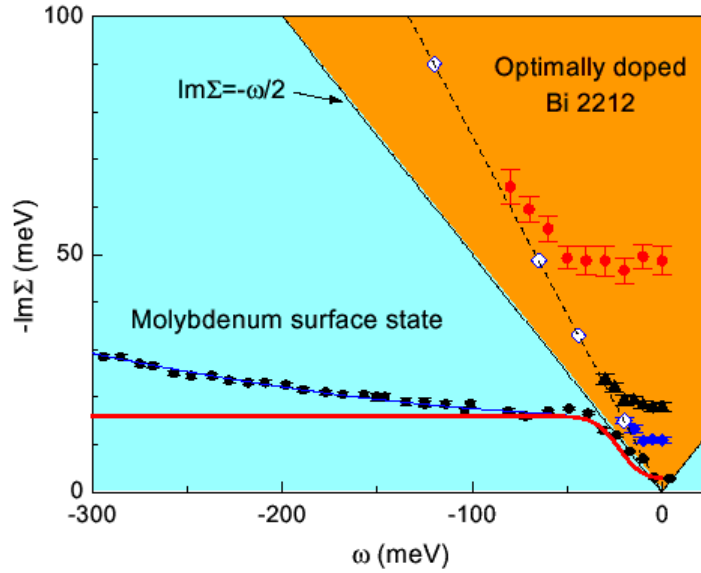


FIGURE 4. Lifetime widths on approaching the Fermi level as measured by angle-resolved photoemission spectroscopy. The testbed results on a Mo(110) surface state (black circles) are well understood in terms of Fermi-liquid theory (blue parabola) and electron phonon interaction (red curve). This is in contrast with results on the superconducting material Bi2212. The red circles, black triangles and blue diamonds correspond to lifetime widths at temperatures 300K, 90K and 48K respectively and lie in a region clearly inconsistent with Fermi liquid behavior. (Courtesy T. Valla)

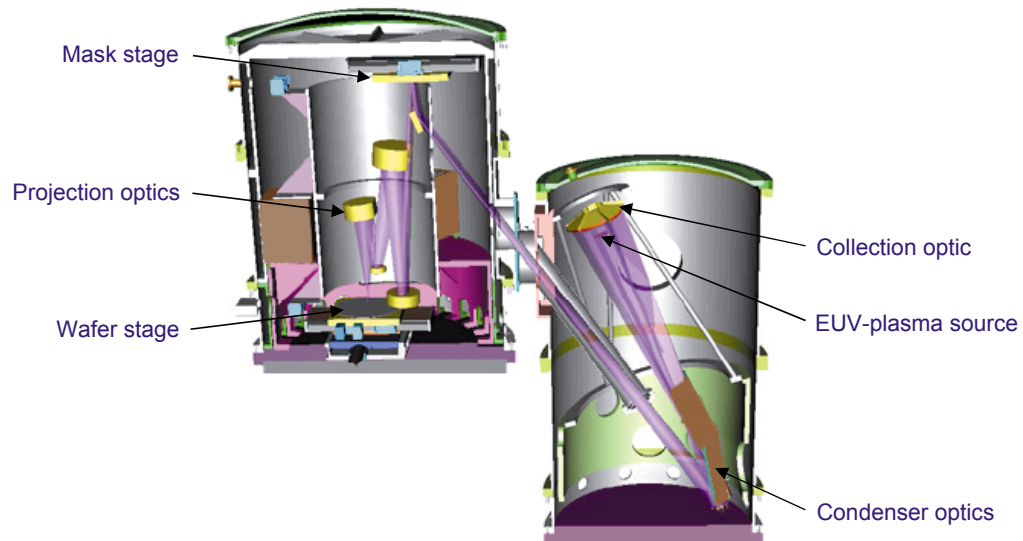
Coherence :

Interferometry for EUV Lithography

According to Moore's famous Law, the density of circuit elements on microchips has doubled roughly every two years, resulting in smaller, faster, and cheaper computers. The present technology, optical lithography, cannot continue indefinitely on this course. The materials from which one could conceivably make lenses, CaF_2 , MgF_2 and LiF will not transmit light at wavelengths less than 100nm. One of the options being considered is to switch from refractive optics to reflective optics, i.e. mirrors. The availability of Mo/Si mirror coatings having reflectances as high as 70% provides special impetus for this technology. The optimum wavelength determined as a compromise between the conflicting requirements of fine lateral spatial resolution and large depth of focus into the chip structure, is about 13nm. This wavelength is popularly referred to as "extreme ultraviolet" or EUV. The corresponding photon energy is 100eV which qualifies as "soft x-ray."

A consortium of microelectronics companies (Intel, Motorola, Advanced Micro Devices) has joined forces with a consortium of National Laboratories (Livermore, Sandia and Berkeley Labs) to build a prototype EUV stepper, an optical camera of the sort to produce small computer chips. A schematic of such a stepper is shown in Figure 5. It comprises a four-mirror optic which produces a demagnified image of the mask on the wafer. The mirrors must be curved and coated with interfering multilayers in order to generate a high reflectivity at 13nm. The EUV source in actual chip manufacture will not be synchrotron radiation but will be derived from an EUV emitting plasma. The role of synchrotron radiation for this technology is optics metrology.

At Berkeley Lab, Jeff Bokor is leading a team that has been entrusted with the task of interferometric characterization of the required high precision mirrors. An old adage says "if you can't measure it, you can't make it." The team has developed an at-wavelength phase-shifting point-diffraction interferometer (PS/PDI) to meet the requisite specifications [9]. The principle of the PS/PDI is to first pass the beam from an ALS undulator through a pinhole to generate a high amplitude perfect spherical wave. A diffraction grating then splits the light into an order (the test beam) which passes through the test optic generating an aberrated wavefront characteristic of the imperfections in the test optic. Another order passes unobstructed through the optic but then is forced through a second pinhole to generate a perfectly spherical reference wavefront which interferes with the test beam. The resulting interferogram reveals the departures from figure accuracy. The design goal was for a test accuracy of 0.10nm over the surface of the mirror. The accuracy actually achieved is 0.05nm. This corresponds to the Bohr radius of a hydrogen atom! A four-mirror optic manufactured at Sandia has already been tested with very satisfactory results. This work demonstrates that coated optics to the desired tolerance can be produced, thereby enhancing the prospects of EUV lithography as the next technology of choice for the manufacture of ever denser microchips.



Courtesy: Richard Stulen, Sandia National Laboratories

FIGURE 5. Schematic representation of an optical system for the manufacture of microchips using EUV projection lithography at 13nm. Multilayer coated mirrors in the stepper create a demagnified image of the mask onto the wafer. A plasma source provides the EUV radiation. (Courtesy R. Stulen, Sandia National Laboratory)

References

1. C. A. Larabell, D. Yager, and W. Meyer-Ilse, in *X-ray Microscopy, Proceedings of the Sixth International Conference*, Berkeley, CA 2-6 August 1999, edited by W. Meyer-Ilse, T. Warwick and D. Attwood, American Institute of Physics, 2000, p. 107.
2. C. Jacobsen, S. Abend, T. Beetz, M. Carlucci-Dayton, M. Feser, K. Kaznacheyev, J. Kirz, J. Maser, U. Neuhausler, A. Osanna, A. Stein, C. Vaa, Y. Wang, B. Winn, S. Wirick, in Ref 1, p.12. D. Weiss, G. Schneider, B. Niemann, P. Guttmann, D. Rudolph, and G. Schmahl, in Ref. 1, p.123.
3. F. Nolting, A. Scholl, J. Stohr, J. Fompeyrine, H. Siegwart, J.-P. Locquet, S. Anders, J. Lüning, E.E. Fullerton, M. F. Toney, M. R. Scheinfein, and H. A. Padmore, *Nature*, **405**, 767 (2000).
4. P.W. Anderson, *Physics Today*, **44** (6), 60 (1991).
5. Z. -X. Shen, D. S. Dessau, B. O. Wells, D. M. King, W. E. Spicer, A. J. Arko, D. Marshall, L.W. Lombardo, A. Kapitulnik, P. Dickinson, S. Doniach, J. DiCarlo, T. Loeser, and C. H. Park, *Phys. Rev. Lett.* **70**, 1553 (1993).
6. J.M. Tranquada, B.J. Sternlieb, J.D. Axe, Y. Nakamura, and S. Uchida, *Nature*, **375**, 561 (1995).
7. Z.J. Zhou, P. Bogdanov, S.A. Kellar, T.Noda, H. Eisaki, S. Uchida, Z.Hussain and Z.-X. Shen, *Science*, **286**, 189 (1999).
8. T. Valla, A.V. Federov, P.D. Johnson. B.O. Wells, S.L. Hulbert, Q. Li, G.D. Gu and N. Koshizuka, *Science*, **285**, 2110 (1999); T. Valla, A.V. Federov, P.D. Johnson and S. L. Hulbert, *Phys. Rev. Lett.*, **83**, 2085 (1999).
9. P. Naulleau, K.A. Goldberg, S. Lee, C. Chang, C. Bresloff, P. Batson, D. Attwood and J. Bokor, *SPIE* **331**, 114 (1998); G. W. Gwyn, R. Stulen, D. Sweeney and D. Attwood, *J. Vac. Sci. Tech.*, **B16**, 3142 (1998).

Affiliation

Neville Smith is Division Deputy for Science at the Advanced Light Source, Lawrence Berkeley National Laboratory.